

Universal short-time behavior of the dynamic fully frustrated XY model

H. J. Luo,* L. Schülke, and B. Zheng

Fachbereich Physik, Universität GH Siegen, D-57068 Siegen, Germany

(Received 16 May 1997; revised manuscript received 4 September 1997)

With Monte Carlo methods we investigate the dynamic relaxation of the fully frustrated XY model in two dimensions below and at the Kosterlitz-Thouless phase transition temperature. Special attention is given to the sublattice structure of the dynamic evolution. The short-time scaling behavior is found and universality confirmed. The critical exponent θ is measured for different temperatures and with different algorithms. [S1063-651X(98)05902-9]

PACS number(s): 64.60.Ht, 75.10.Hk, 02.70.Lq, 82.20.Mj

I. INTRODUCTION

There has been a long history of the study of the universal scaling behavior for critical dynamics. It is well known that there exists a universal scaling form when dynamic systems reach equilibrium or in the long-time regime of their dynamic evolution. When a dynamic magnetic system has evolved for a sufficiently long time, the magnetization decays exponentially. The characteristic time scale for this regime is $t_\tau \sim \tau^{-\nu z}$ or $t_L \sim L^z$, with τ being the reduced temperature and L being the lattice size. Before this exponential decay the time evolution of the magnetization obeys a power law $t^{-\beta/\nu z}$. All this universal scaling behavior can be characterized by a set of three critical exponents: two static exponents β, ν and one dynamic exponent z .

Is there universal behavior in the *short-time regime* of the dynamic evolution? For long, the answer had been no. It was believed that the behavior of the dynamic systems in the short-time regime depends essentially on the microscopic details. However, it has been discovered recently that universal scaling behavior emerges already in the *macroscopic* short-time regime, after a microscopic time scale t_{mic} [1]. Important is that extra critical exponents should be introduced to describe the dependence of the scaling behavior on the initial conditions [1,2] or to characterize the scaling behavior of special dynamic observables [3–5]. A typical dynamic process is that a magnetic system initially at *high temperature with a small initial magnetization* is suddenly quenched to the critical temperature (without any external magnetic field) and then released to the time evolution with a dynamics of model A [6]. A new dynamic exponent x_0 has been introduced to describe the scaling dimension of the initial magnetization. More surprisingly, at the beginning of the time evolution the magnetization undergoes a critical initial increase [1,7,8]

$$M(t) \sim m_0 t^\theta, \quad (1)$$

where θ is related to the scaling dimension x_0 of the initial magnetization m_0 by $\theta = (x_0 - \beta/\nu)/z$.

The physical background for the initial increase of the magnetization is not completely clear. The critical initial increase has little to do with the symmetry breaking below the critical temperature. Actually similar phenomena can be observed even in the case where the magnetization is not an order parameter. For the six-state clock model and the XY model, below the Kosterlitz-Thouless phase transition temperature no real long-range order appears. The normal magnetization is not an order parameter here. However, the power-law initial increase is still observed in numerical simulations [9,10].

On the other hand, in recent years much attention has been put on statistical systems with frustrations or quenched randomness. The critical behavior of these systems often is quite different from that of regular systems. Due to the severe critical slowing down, numerical simulations of these systems are extremely difficult. In particular, our knowledge of the dynamic properties of these systems is poor.

In this paper, as an approach to the short-time dynamics of statistical systems with frustrations, we investigate numerically the dynamic fully frustrated XY model below or at the Kosterlitz-Thouless phase transition temperature. We concentrate our attention on the scaling behavior of the magnetization and its dependence on the initial value. Much effort is devoted to the understanding of the special properties induced by the sublattice structure of the ground states. The investigation of the universal short-time behavior of the dynamic systems is important not only conceptually but also in the practical sense. Numerical simulations for the Ising and Potts models show that we may obtain already from the short-time dynamics the static critical exponents as well as the dynamic exponent z , which are normally defined and measured in equilibrium or in the long-time regime of the dynamic evolution [8,11,12,9,13,14]. Since our measurements in the short-time dynamics are always carried out at the beginning of the time evolution and the average is really a sample average rather than a time average based on the ergodicity assumption as in the measurements in equilibrium, the dynamic approach might be free of critical slowing down.

In the next section the fully frustrated XY model is briefly introduced. In Secs. III and IV numerical results are reported for the dynamic fully frustrated XY model. Finally conclusions follow in Sec. V.

*On leave from Sichuan Union University, Chengdu, People's Republic of China.

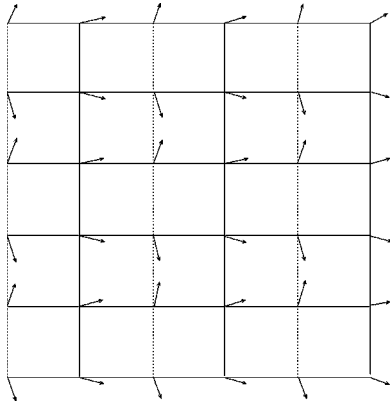


FIG. 1. One of the ground states for the FFXY model. Dotted lines denote negative links.

II. THE FULLY FRUSTRATED XY MODEL

The fully frustrated XY (FFXY) model in two dimensions can be defined by the Hamiltonian

$$H = K \sum_{\langle ij \rangle} f_{ij} \vec{S}_i \cdot \vec{S}_j, \quad (2)$$

where $\vec{S}_i = (S_{i,x}, S_{i,y})$ is a planar unit vector at site i and the sum is over the nearest neighbors. In our notation the factor $1/kT$ has been absorbed in the coupling K . Here f_{ij} takes the value $+1$ or -1 , depending on the links. A simple realization of the FFXY model is by taking $f_{ij} = -1$ on half of the vertical links (negative links) and others are $+1$ (positive links). This is shown in Fig. 1. The links marked by dotted lines represent the negative links.

There exist two phase transitions in the FFXY model: the Kosterlitz-Thouless phase transition (XY -like) and the second-order phase transition (Ising-like). This is very different from the regular XY model. Much effort has been made to locate the critical points for both transitions and measure the corresponding critical exponents. In a recent paper [15], it is reported that the XY -like phase transition temperature is $T_{KT} = 1/K_{KT} = 0.446$, while the Ising-like phase transition temperature $T_c = 1/K_c = 0.452$. The measurements show a slight difference of these two phase transition temperatures. Earlier results for the FFXY model and its ordering dynamics could be found in Refs. [16–24].

One of the most important properties of the fully frustrated XY model is its sublattice structure of the ground states. In the regular XY model, in the ground state all spins orient in the same direction. However, for the FFXY model the lattice should be divided into four sublattices. All spins in each sublattice orient in the same direction, but the directions for the four sublattices are different and connected in a certain way, as it is shown in Fig. 1. For the whole lattice, the ground state preserves the global $O(2)$ symmetry, i.e., spins can rotate *globally*. No real long-range XY -like order emerges in the FFXY model. This situation is similar to the regular XY model. In addition to the ground state shown in Fig. 1, there is another ground state that is obtained by translating the configuration in Fig. 1 by one lattice spacing in the

y direction. Below the Ising-like critical temperature T_c , this Z_2 symmetry is broken. The second-order phase transition occurs.

In this paper we study the short-time dynamic properties of the FFXY model below and at the XY -like phase transition temperature T_{KT} . Below the critical temperature T_{KT} , the FFXY model remains critical in the sense that the correlation length keeps divergent. Therefore, a scaling form is expected even below the critical temperature T_{KT} . However, the critical exponents may vary with respect to the temperature. Such a phenomenon has been observed in the six-state clock model and the regular XY model [9,10]. The dynamic properties related to the Ising-like phase transition will not be discussed in this paper.

III. SUBLATTICE STRUCTURE OF DYNAMIC EVOLUTION

Let us consider a dynamic relaxation process starting from an initial state with a *very high temperature and small magnetization* [1]. As a direct generalization of the XY model, for the FFXY model the magnetization may also be defined as

$$\vec{M}(t) = \frac{1}{L^2} \sum_i \vec{S}_i, \quad (3)$$

with L being the lattice size. As in case of the XY model, the magnetization here is also not an order parameter. To achieve an initial magnetization, we introduce an initial external magnetic field, e.g., in the x direction [10]. Suppose the initial state is at a very high temperature. The initial Hamiltonian can be written as

$$H_0 = 2h \sum_i S_{i,x}. \quad (4)$$

Here the factor $1/kT$ already has been absorbed in h and the interaction between spins is ignored due to the very high temperature. With this initial Hamiltonian H_0 , we update the initial system by use of the Metropolis algorithm until it reaches equilibrium. Then the configurations generated in this way are used as initial configurations of the dynamic system. The initial magnetization generated is

$$\vec{M}(0) = (m_0, 0) \approx (h, 0), \quad h \rightarrow 0. \quad (5)$$

There are, of course, many other methods to generate an initial magnetization. However, it has been demonstrated that the universal behavior does not depend on these microscopic details, i.e., how a magnetization is constructed [10]. Effects of the microscopic details of the initial configurations are swept away in almost one Monte Carlo time step.

After the preparation of an initial configuration, the external magnetic field h is removed and the system is released to a dynamic evolution of model A below or at the XY -like transition temperature. In this paper, *the Metropolis algorithm* is mainly used. To confirm universality, however, some simulations are repeated with the heat-bath algorithm in some special cases. We stop updating the dynamic system after 150 Monte Carlo time steps and repeat the procedure

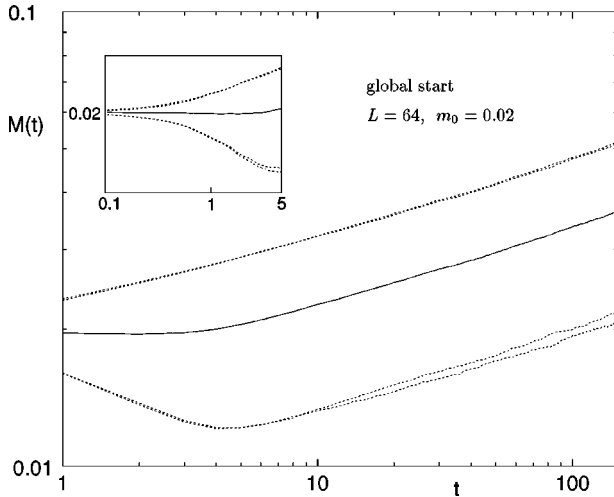


FIG. 2. Time evolution of the magnetization with the global start for $L=64$ and $m_0=0.02$ with the Metropolis algorithm plotted on a double-logarithmic scale. $M(t)$ is the x component of the magnetization $\vec{M}(t)$ defined in Eq. (3) and the time unit is defined as a Monte Carlo sweep over all sites of the lattice. The solid line represents the global magnetization, while dotted lines are those for the four sublattices. The inset shows the behavior for very small time t .

with another initial configuration. The average is over both the independent initial configurations and the random numbers. We have performed simulations with lattice sizes $L=8, 16, 32, 64,$ and 128 . Total samples for the average are from 30 000 to 60 000, depending on lattice sizes, initial states, and algorithms. Errors are estimated by dividing the samples into three or four groups.

In Fig. 2 the time evolution of the magnetization is displayed on a double-logarithmic scale with a solid line for the lattice size $L=64$ and the initial magnetization $m_0=0.02$. The temperature is taken to be $T=0.400$, which is slightly below the XY -like transition temperature $T_{KT}=0.446$ given in Ref. [15] (or $T_{KT}=0.440(2)$ in [20]). In the figure $M(t)$ is the x component of the magnetization $\vec{M}(t)$. The y component of the magnetization $\vec{M}(t)$ remains zero since the initial value is zero. The inset shows the behavior of the magnetization at the very beginning of the time evolution. Here a Monte Carlo sweep over all sites on the lattice is defined as the time unit. From the figure we see that the magnetization keeps more or less constant for two or three time steps and then increases indeed. The universal power-law behavior becomes apparent after about 20–30 Monte Carlo time steps. From the slope of the curve, one measures the exponent $\theta=0.184(6)$. In this simulation a global uniform initial external magnetic field h has been applied to the whole lattice or, in other words, the initial magnetization density distribution is uniformly generated. We call this the *global start*.

Does the sublattice structure of the ground state play some role in the dynamic evolution? In equilibrium, it is known that the XY susceptibility should be calculated separately for each sublattice since the orientations of spins in different sublattices differ. However, further understanding of the sublattice structure in numerical simulations cannot so easily be achieved due to the $O(2)$ symmetry and large fluctuations. In the short-time dynamics, the situation is some-

what different. The $O(2)$ symmetry is violated by the initial magnetization. One can really measure the time evolution of the magnetization separately for each sublattice shown in Fig. 1. The two upper dotted lines in Fig. 2 represent the time evolution of the magnetization for the two sublattices connected to the positive links, while the lower two dotted lines are those for two sublattices connected to the negative links. It is very interesting that even though we have a global start, for sublattices connected to the positive links the magnetizations *increase* from the beginning, while for sublattices connected to the negative links they *drop essentially* in the first time steps. This can be seen clearly from the small window in the figure. After about 5 Monte Carlo steps, the magnetizations on the negative links begin to increase. Within 20–30 Monte Carlo time steps, all the magnetizations, either on the positive links or on the negative links, tend to the *same* universal power-law behavior even though their magnitudes remain different.

This means that the microscopic time scale for our system is $t_{mic} \sim 20-30$. The behavior of the dynamic system within t_{mic} is *not* universal. It depends on microscopic details, e.g., initial configurations, algorithms, updating schemes, lattice types, and the interaction, as well as on which sublattice the observable is measured. The universal power-law behavior in Eq. (1) does not apply in this time period.

Without an external magnetic field, the magnetization in equilibrium should be zero. One would naturally ask how long the initial increase of the magnetization will last and how $M(t)$ goes to zero after the initial increase. A systematic analysis of this has been given, for example, for the Ising systems in Refs. [25,7]. The time scale for the critical initial increase is proportional to $t_0 \sim m_0^{-z/\nu}$. After that, the magnetization crosses over to the power-law decay $t^{-\beta/\nu z}$ and then finally to the exponential decrease in the long-time regime of the dynamic evolution. The time scale t_0 becomes infinite in the limit $m_0=0$ and therefore the initial magnetization can also leave its trace in the long-time regime. Actually, the time period for the critical initial increase is already very long even for a finite m_0 . To show this, we have carried out a simulation for the FFX model up to 20 000 Monte Carlo steps with $m_0=0.1$. A large lattice size $L=256$ has been taken in order to avoid finite-size effects. The result is shown in Fig. 3. The lower solid line represents the global magnetization, while the upper and lower dotted lines are those for the averaged magnetizations on the positive links and the negative links, respectively. Here we see that even for a not so small value $m_0=0.1$, the magnetizations keep the power-law increase until a time between 1000 and 2000 Monte Carlo steps. After that the magnetizations begin to deviate from the power law. From this, we may also realize how difficult it is to generate independent configurations. The numerical simulation of the FFX model in traditional ways is essentially hampered by a critical slowing down.

Now we return to the sublattice structure of the dynamic evolution. What is the relation between the magnetizations on the positive links and the negative links? In Fig. 4 the ratio $r(t)$ of the magnetization averaged over the two sublattices on the positive links and that on the negative links is plotted with a solid line. The data are taken from those of Fig. 2. The ratio $r(t)$ stabilizes to a constant value very quickly within 10 time steps. Averaging this ratio in a time

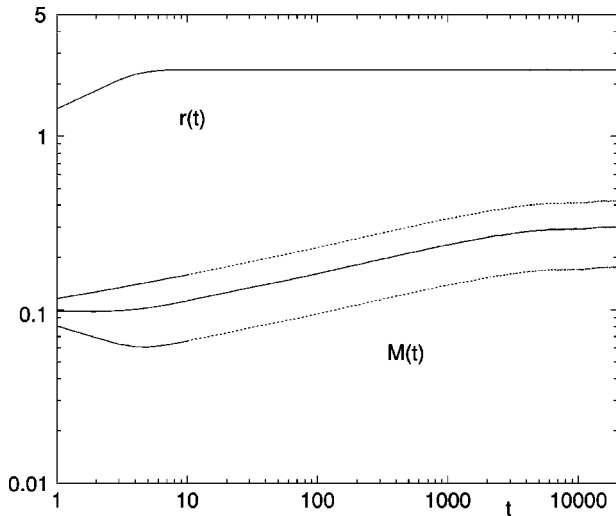


FIG. 3. Time evolution of the magnetization with the global start for $L=256$ and $m_0=0.1$ with the Metropolis algorithm plotted on a double-logarithmic scale. The lower solid line represents the global magnetization. The two dotted lines are the magnetizations for the positive links and the negative links, and the upper solid line is the ratio $r(t)$ of these two.

interval $[10,150]$, we get $r=2.4147(8)$. What is this ratio? In the ground state drawn in Fig. 1, the angles between spins on the positive links and the x axis is $\pm\pi/8$, while those between spins on the negative links and the x axis are $\pm 3\pi/8$. The ratio r is nothing but the ratio of the x components of the spins on both the positive links and the negative links. We see this by calculating $r_{th} = \cos(\pi/8)/\cos(3\pi/8) = 2.4142$. The consistence between r_{th} and the measured one $r=2.4147(8)$ is remarkable.

The fact that r takes a constant value as in the ground state does not depend on the initial value of the magnetization. It is also not a property only in the initial stage of the time evolution. In Fig. 3 the upper solid line shows the ratio $r(t)$ measured in the simulation for $L=256$ with $m_0=0.1$ and up to the time steps 20 000. We can see that the $r(t)$ keeps a constant value around r_{th} until the time limit of our simulation where the magnetization $M(t)$ has already devi-

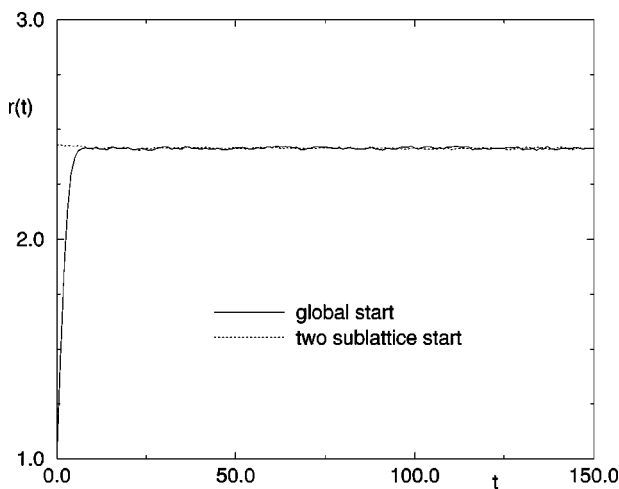


FIG. 4. Ratio $r(t)$ for different initial states.

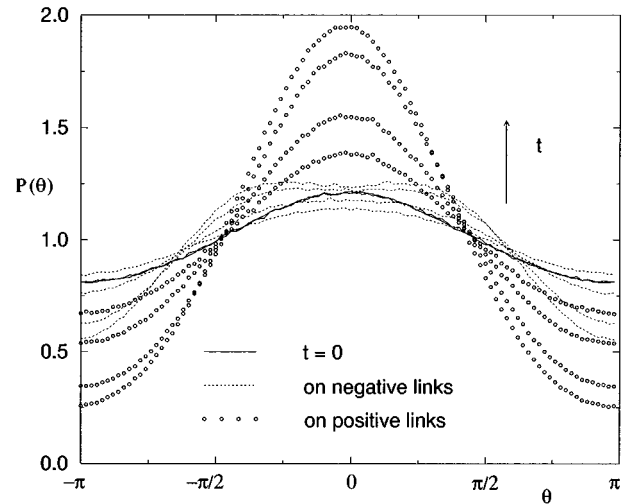


FIG. 5. Time evolution of the angular distribution $P(\theta)$ of spins on positive links (represented by the circled lines) and on negative links (represented by dotted lines). From bottom to top (looking at the central part of the curves), the four lines represent distributions at 20, 200, 2000, and 20 000 Monte Carlo time steps, respectively, for both kinds of links. The two overlapping solid lines are those for $t=0$. The scale for $P(\theta)$ is chosen in such a way that for spins distributed homogeneously in all directions $P(\theta)\equiv 1$ for $\theta\in[-\pi, \pi]$.

ated from the power-law increase as shown in the same figure. For a better understanding of the phenomenon, we have also measured the evolution of the angular distribution $P(\theta)$ of the spins in the simulation. The angle θ is that between the spin and the x direction. In Fig. 5 two solid lines are the initial angular distributions for the spins on the positive and negative links. They show Gaussian-like shape with peaks at zero. For increasing time both distributions behave quite differently: The distribution on the positive links becomes sharper, while in contrast to that the distribution on the negative links becomes flatter, where the peak value even decreases during the first time steps below $t=20$, and then with increasing time the distribution gradually splits into two peaks. Although this behavior might reflect some effect of the ground state, the results show that the spin configurations in the dynamic system are not the same as those of the ground state. How can the behavior of $r(t)$ be explained? Our argument is that this is due to a similar scaling behavior of the magnetizations on positive links $[M_p(t)]$ and on negative links $[M_n(t)]$. According to Janssen, Schaub, and Schmittmann [1], the scaling relation of the magnetization below the critical temperature T_{KT} is

$$M(t, m_0) = b^{-\eta/2} M(b^{-z}t, b^{x_0}m_0). \quad (6)$$

For two-dimensional XY systems the anomalous dimension is written as $\eta/2$. Due to the scaling relation $\eta/2$ is equal to β/ν in two-dimensional Ising systems. The dynamic exponent z for the XY systems below the critical temperature T_{KT} is defined as the scaling dimension of the dynamic variable t . If we suppose that this scaling relation also holds for $M_p(t)$ and $M_n(t)$ separately, choosing $b=t^{1/z}$ we easily get

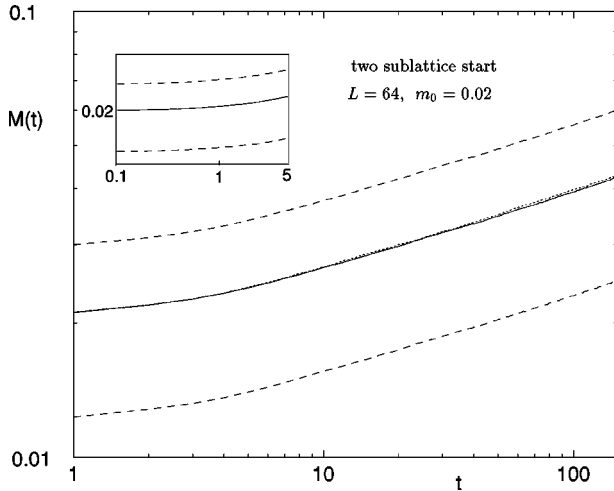


FIG. 6. Time evolution of the magnetization with the two-sublattice start for $L=64$ and $m_0=0.02$ with the Metropolis algorithm plotted on a double-logarithmic scale. $M(t)$ is the x component of the magnetization $\vec{M}(t)$. The solid line represents the global magnetization, while the dashed lines are those for the sublattices. For comparison, the dotted line is the global magnetization with the sharp preparation of the initial magnetizations. The inset describes the behavior of the magnetization at the very beginning of the evolution.

$$r(t) = \frac{M_p(t, m_0)}{M_n(t, m_0)} = F(m_0 t^{x_0/z}). \quad (7)$$

As a function of $m_0 t^{x_0/z}$, if $r(t)$ does not depend on t , it should also not depend on m_0 . Further, $r(t)$ should not depend on the temperature when the temperature is below T_{KT} , according to the scaling form (7). In the limit $T=0$, the spin configuration will be apparently frozen in the ground state. Therefore, $r(t)$ takes the constant value as in the ground state.

To understand more about the effect of the initial configuration, we now divide the lattice into *two* sublattices: the sublattice on the positive links and the one on the negative links. We have performed a simulation with different initial magnetizations for the two sublattices, m_{0p} and m_{0n} , respectively. We take, for example, $m_{0p}/m_{0n}=r_{th}$ and keep the global initial magnetization $m_0=0.02$. We call this the *two-sublattice start*.

The way to prepare such initial configurations is similar to that of the global start. The difference is that the initial external magnetic field for the spins on positive links is h_p and that on negative links is h_n . Both are in the x direction and the ratio h_p/h_n is chosen to be r_{th} . The time-dependent magnetizations with this initial condition are plotted in Fig. 6. The solid line is the global magnetization, while the upper and lower dashed lines represent those for the sublattices on the positive links and negative links, respectively. Now the initial drop for the magnetization on the negative links disappears. The corresponding ratio $r(t)$ is plotted also in Fig. 4 with the dotted line. It remains constant from almost the very beginning of the time evolution. The averaged value is $r=2.4146(6)$. However, the time period for the magnetization

to enter the universal power-law behavior is again 20–30, almost the same as that in Fig. 2.

Before going further we would like to mention the problem of the *sharp preparation* of the initial magnetization. If the lattice size is infinity, in each initial configuration generated by the initial Hamiltonian H_0 , an exact value $(m_0, 0)$ of the initial magnetization $\vec{M}(0)$ is automatically achieved. However, the practical lattice size is finite and the initial magnetization $\vec{M}(0)$ fluctuates around $(m_0, 0)$. This is a kind of extra finite-size effect. It causes a problem in a high-precision measurement. In order to reduce this effect, a sharp preparation technique has been introduced [7,8,26]. How important the sharp preparation is depends on the initial magnetization m_0 and what kind of observables one measures. The smaller the initial magnetization m_0 , the more important the sharp preparation becomes. In Fig. 6 the result for the time evolution of the magnetization with the sharp preparation technique has been plotted with the dotted line. The curve almost overlaps with that without the sharp preparation technique. This shows that the extra finite-size effect here is already quite small for the lattice size $L=64$. For simplicity, our simulations are always carried out with no sharp preparation of the initial magnetization.

Now we go a step further. From the numerical simulations shown in Figs. 2, 4, and 6 and the discussions above, we understand that the universal behavior of the dynamic system is closely related to the structure of the ground states. If the initial state is completely random with zero initial magnetization, the probabilities for the magnetization to evolve to different directions are the same and the averaged magnetization remains zero. However, if a nonzero initial magnetization is given in a certain direction, the time-dependent magnetization grows in this direction since the energy is in favor of it. To clarify this point, we start with an initial state that is even closer to the ground state. We prepare different initial magnetizations for the *four* sublattices, aligning them parallel to the spins in the ground state shown in Fig. 1. All the magnitudes of the initial magnetizations are $m_0=0.02$. We call this initial state the *four sublattice start*. The time evolution of the magnetizations for different sublattices is shown in Fig. 7. Here $M(t)$ is just the projection of the magnetization in the direction of the initial magnetization in each sublattice. The solid line and dotted line are the magnetizations for the sublattices on the positive links, while the circles and crosses are those on the negative links. They collapse on a single line and show completely the same universal behavior.

In Table I values for the critical exponent θ measured in a time interval [40,150] for the three different initial states are collected. Within the statistical errors they are consistent.

IV. UNIVERSALITY AND SCALING

In the numerical measurement of the critical exponent θ we should pay attention to two possible effects: the finite-size effect and the finite- m_0 effect. For the dynamic process discussed in the preceding section, there are two kinds of finite-size effects. One is the extra finite-size effect from the initial configurations. This extra finite-size effect is closely related to the problem of the sharp preparation of the initial configurations and was discussed in Sec. III.

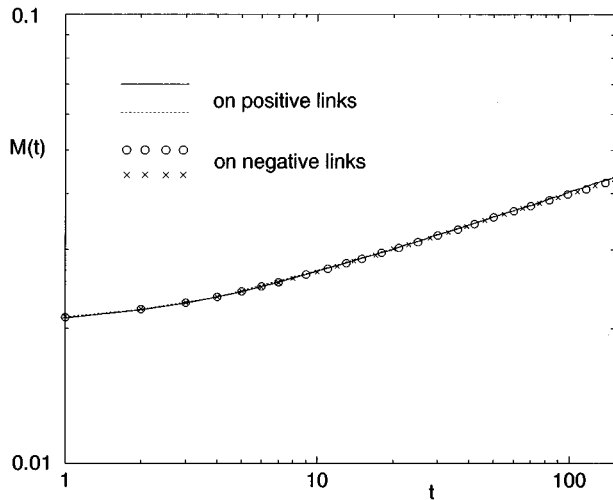


FIG. 7. Time evolution of the magnetization with the four-sublattice start for $L=64$ and $m_0=0.02$ with the Metropolis algorithm plotted on a double-logarithmic scale. $M(t)$ is the projection of the magnetization $\vec{M}(t)$ on the initial direction. The solid and dotted line are the magnetizations for the sublattices on the positive links, while the circles and crosses represent those on the negative links.

Another kind of finite-size effect is the normal finite-size effect that takes place in a time scale $t_L \sim L^z$. Whenever the system evolves into this time regime, the magnetization will decay by an exponential law $\exp(-t/t_L)$. In order to see the normal finite-size effect, we have plotted on a double-logarithmic scale the time evolution of the magnetization for the lattice sizes $L=8, 16, 32, 64$, and 128 with initial magnetization $m_0=0.02$ in Fig. 8. The upper solid line is the time-dependent magnetization for $L=64$, while the dotted lines are those for $L=8, 16, 32$, and 128 , respectively. The curves for $L=64$ and $L=128$ more or less overlap. The values for the critical exponent θ are $\theta=0.181(5)$ and $0.182(3)$ for $L=64$ and $L=128$, respectively. Therefore, we conclude that the finite-size effect here is already negligibly small for the lattice size $L=64$.

Rigorously speaking, the critical exponent is defined in the limit $m_0=0$. However, it is practically only possible to perform the measurement with a finite m_0 . The exponent θ measured may show some dependence on the initial magnetization m_0 . In general, an extrapolation (linear or nonlinear) to the limit of $m_0=0$ should be carried out [8,26]. For this purpose, we perform another simulation for the lattice size $L=64$ and with an initial magnetization $m_0=0.01$. The time-

TABLE I. Exponent θ measured for lattice size $L=64$ with different types of initial configurations and algorithms. I, II, and III represent initial states of the global start, two sublattice start, and four sublattice start.

| | Metropolis | | | Heat bath |
|--|------------|----------|----------|-----------|
| | I | II | III | II |
| | 0.184(6) | 0.182(5) | 0.181(5) | 0.186(6) |

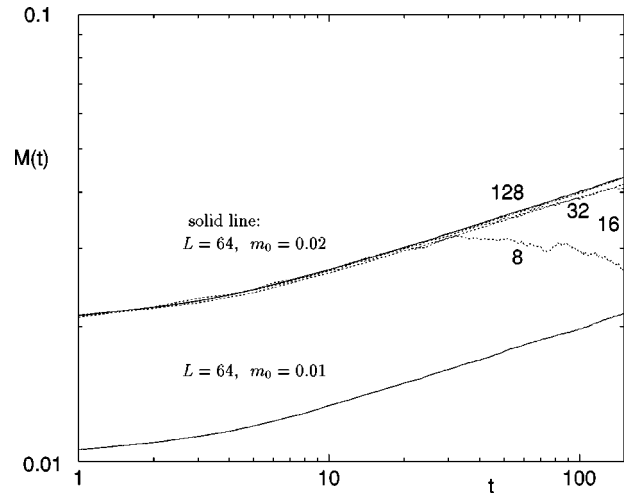


FIG. 8. Time evolution of the magnetization with the four-sublattice start for different L and m_0 with the Metropolis algorithm plotted on a double-logarithmic scale. $M(t)$ is the projection of the magnetization $\vec{M}(t)$ in the initial direction. The solid line represents the magnetization for $L=64$, while dotted lines are those for other lattice sizes.

dependent magnetization is also displayed with the lower solid line in Fig. 8. The values for the exponent θ obtained for $m_0=0.02$ and $m_0=0.01$ are $\theta=0.181(5)$ and $0.179(7)$, respectively. Within the statistical errors, they cover each other. The dependence of the exponent θ on m_0 is already rather weak here; an extrapolation is not necessary. This is also the reason why the results with and without the sharp preparation of the initial magnetization are not so different. In the further discussion in this paper we will restrict ourselves mostly to $L=64$ and $m_0=0.02$.

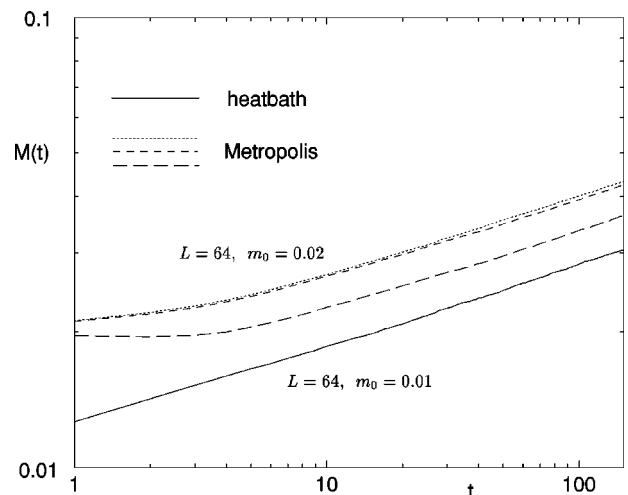


FIG. 9. Time evolution of the magnetization for different initial states and algorithms plotted on a double-logarithmic scale. $M(t)$ is the projection of the magnetization $\vec{M}(t)$ in the initial direction. The solid line represents the magnetization for $L=64$ and $m_0=0.01$ with the heat-bath algorithm and the two-sublattice start, while long-dashed, dashed, and dotted lines are those for $L=64$ and $m_0=0.02$ with the Metropolis algorithm for the global, two-sublattice, and four-sublattice starts, respectively.

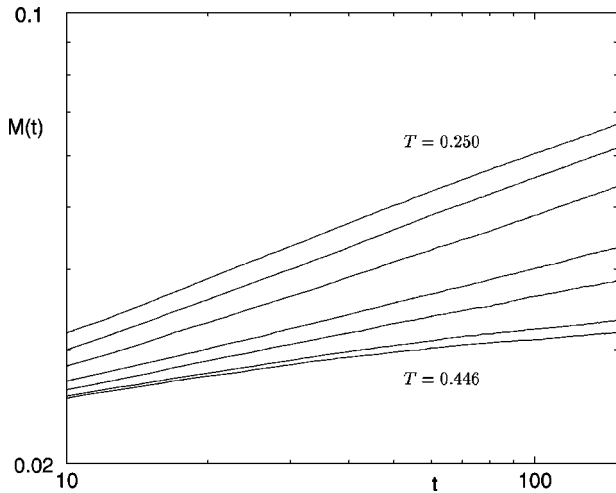


FIG. 10. Time evolution of the magnetization for $L=64$ and $m_0=0.02$ with different temperatures plotted on a double-logarithmic scale. The four-sublattice start and the Metropolis algorithm are used in the simulations. $M(t)$ is the projection of the magnetization $\vec{M}(t)$ in the initial direction. From top to bottom, the temperature is $T=0.250, 0.300, 0.350, 0.400, 0.420, 0.440,$ and 0.446 , respectively.

Is the power-law scaling behavior in Eq. (1) for the magnetization really universal? For example, can it depend on the microscopic details of the initial state, the algorithms, the lattice types, or even the additional non-nearest interactions? Many discussions of this kind have been made recently [26,27,10,4,28]. Here we have also repeated some calculations with the heat-bath algorithm to confirm universality. The result for $L=64$ and $m_0=0.02$ with the two-sublattice start is plotted in Fig. 9 with the solid line. The initial magnetizations m_{0p} and m_{0n} are given to the sublattices on the positive links and the negative links, respectively, with $m_{0p}/m_{0n}=r_{th}=2.4142$. The long-dashed, dashed, and dotted line are the results with the Metropolis algorithm with the global start, the two-sublattice start, and the four-sublattice start, respectively. All the measured values for the corresponding exponent θ are listed in Table I. The fact that all the four curves give consistent values for the exponent θ within the statistical errors provides strong support for universality. In particular, that the exponent θ is independent of the initial states indicates that some physical mechanism closely related to the ground states essentially governs the time evolution of the dynamic systems.

To understand universality in the short-time dynamics, we keep in mind that there are two very different time scales in the dynamic systems: the microscopic time scale and the macroscopic time scale. The typical macroscopic time scale is t_τ or t_L . Universal behavior emerges only after a sufficiently long time period in the microscopic sense. Such a time period that the dynamic system needs to sweep away the microscopic behavior is called t_{mic} . One expects that the time scale t_{mic} is still very short in the macroscopic sense. In numerical simulations, a Monte Carlo time step can be considered as a typical microscopic unit. Most numerical simulations for dynamic systems show that $t_{mic} \sim 10-50$. In Fig. 9 we see that this is also the case for the FFXY model. These

TABLE II. Exponent θ measured for different temperatures with the Metropolis algorithm. The lattice size is $L=64$.

| T | θ |
|-------|----------|
| 0.446 | 0.060(7) |
| 0.440 | 0.079(4) |
| 0.420 | 0.141(5) |
| 0.400 | 0.181(5) |
| 0.350 | 0.245(3) |
| 0.300 | 0.263(2) |
| 0.250 | 0.260(2) |

results are reasonable. Compared to the typical macroscopic time scale t_τ or t_L , the microscopic time scale t_{mic} observed in numerical simulations is indeed very small. In some cases, universal behavior emerges actually in one Monte Carlo time step, e.g., in the numerical measurement of the critical exponent θ for the two-dimensional Potts model [8,26]. Such a clean behavior in the very-short-time regime is somehow unexpected.

It is well known that for the XY-like phase transition no real long-order emerges even below the transition temperature T_{KT} . The system remains critical in the sense that the correlation length is divergent. A similar scaling behavior is expected for any temperature below T_{KT} . However, the critical exponents may vary with respect to the temperature. In Fig. 10 the time evolution of the magnetization for different temperatures is displayed. We clearly see there exists power-law behavior for all the temperatures below T_{KT} . However, the critical exponent θ varies essentially as can be seen from the results given in Table II. The dependence of the critical exponent θ on the temperature for the FFXY model is qualitatively the same but stronger than that for the regular XY model [10]. As the temperature decreases, the exponent θ first increases and then slowly decreases. At the XY-like transition temperature $T_{KT}=0.446$ [15] [or 0.440(2) in Ref. [20]], the exponent $\theta=0.060(7)$ is quite small compared to $\theta=0.250(1)$ for the XY model at the critical temperature $T_{KT}=0.90$. Therefore, the power-law behavior around the critical temperature T_{KT} is less prominent compared to that for the XY model and also that at the lower temperature. We have performed some simulations with temperatures above T_{KT} too. Since the correlation length is divergent *exponentially* when the temperature approaches from above the XY-like transition point, however, no rigorous information for the XY-like transition temperature T_{KT} could be obtained from our data. Further investigation along this direction is needed.

V. CONCLUSIONS

We have numerically simulated the dynamic relaxation process of the fully frustrated XY model in two dimensions starting from an initial state with a very high temperature and small initial magnetization. Special attention has been put on the sublattice structure of the dynamic evolution induced by the ground state. The universal power-law behavior is found

independently of the sublattice structure of the initial states. The critical exponent θ has been measured for different temperatures below T_{KT} . Universality has been further confirmed by carrying out the simulations with both the Metropolis and the heat-bath algorithm. Many important problems remain open in connection to the present paper, e.g., the short-time behavior of the dynamic FFXY model with respect to the Ising-like phase transition and the deter-

mination of the critical point as well as other critical exponents from the short-time dynamics.

ACKNOWLEDGMENTS

H.J.L. would like to thank the Heinrich Hertz Stiftung Foundation for financial support. This work was supported in part by the Deutsche Forschungsgemeinschaft under Grant No. DFG Schu 95/9-1.

-
- [1] H. K. Janssen, B. Schaub, and B. Schmittmann, *Z. Phys. B* **73**, 539 (1989).
 - [2] D. A. Huse, *Phys. Rev. B* **40**, 304 (1989).
 - [3] S. N. Majumdar, C. Sir, A. J. Bray, and S. Cornell, *Phys. Rev. Lett.* **77**, 2867 (1996).
 - [4] L. Schülke and B. Zheng, *Phys. Lett. A* **233**, 93 (1997).
 - [5] K. Oerding, S. J. Cornell, and A. J. Bray, *Phys. Rev. E* **56**, R25 (1997).
 - [6] P. C. Hohenberg and B. I. Halperin, *Rev. Mod. Phys.* **49**, 435 (1977).
 - [7] Z. B. Li, U. Ritschel, and B. Zheng, *J. Phys. A* **27**, L837 (1994).
 - [8] L. Schülke and B. Zheng, *Phys. Lett. A* **204**, 295 (1995).
 - [9] P. Czermer and U. Ritschel, *Phys. Rev. E* **53**, 3333 (1996).
 - [10] K. Okano, L. Schülke, K. Yamagishi, and B. Zheng, *J. Phys. A* **30**, 4527 (1997).
 - [11] L. Schülke and B. Zheng, *Phys. Lett. A* **215**, 81 (1996).
 - [12] P. Grassberger, *Physica A* **214**, 547 (1995).
 - [13] Z. B. Li, L. Schülke, and B. Zheng, *Phys. Rev. Lett.* **74**, 3396 (1995).
 - [14] Z. B. Li, L. Schülke, and B. Zheng, *Phys. Rev. E* **53**, 2940 (1996).
 - [15] P. Olsson, *Phys. Rev. Lett.* **75**, 2758 (1995).
 - [16] A. Scheinine, *Phys. Rev. B* **39**, 9368 (1989).
 - [17] J. Lee, J. M. Kosterlitz, and E. Granato, *Phys. Rev. B* **43**, 11 531 (1991).
 - [18] D. B. Nicolaides, *J. Phys. A* **24**, L231 (1991).
 - [19] G. Ramirez-Santiago and F. V. José, *Phys. Rev. Lett.* **68**, 1224 (1992).
 - [20] S. Lee and K. Lee, *Phys. Rev. B* **49**, 15 184 (1994).
 - [21] S. J. Lee, J. R. Lee, and B. Kim, *Phys. Rev. E* **51**, R4 (1995).
 - [22] J. Villain, *J. Phys. C* **10**, 1717 (1977); **10**, 4793 (1977).
 - [23] S. Teitel and C. Jayaprakash, *Phys. Rev. B* **20**, 3761 (1979).
 - [24] S. Miyashita and H. Shiba, *J. Phys. Soc. Jpn.* **53**, 1145 (1984).
 - [25] H. W. Diehl and U. Ritschel, *J. Stat. Phys.* **73**, 1 (1993).
 - [26] K. Okano, L. Schülke, K. Yamagishi, and B. Zheng, *Nucl. Phys. B* **485**, 727 (1997).
 - [27] L. Schülke and B. Zheng, in *Proceeding of the XIVth International Symposium on Lattice Field Theory* [*Nucl. Phys. B, Proc. Suppl.* **53**, 712 (1997)].
 - [28] X. W. Liu and Z. B. Li, *Commun. Theor. Phys.* **27**, 511 (1997).